JOURNAL OF THERMOPHYSICS AND HEAT TRANSFER
Vol. 24, No. 3, July–September 2010

Heat Balance of a Transpiration-Cooled Heat Shield

Hannah Böhrk,* Olivier Piol,† and Markus Kuhn*
DLR, German Aerospace Center, 70569 Stuttgart, Germany

DOI: 10.2514/1.47172

HEATS is a layout tool for the determination of transient wall heat flux to a transpiration-cooled parallel flat plate under laminar or turbulent flow conditions. The method is based on heat balances between wall material, transpired coolant, and surrounding hot gas. It is introduced here with particular focus on a reentry mission. The investigation of transpiration cooling necessitates considering the entire flight trajectory. Because of long calculation times, computational fluid dynamics tools cannot be used. The calculation of wall temperatures of an entire trajectory with HEATS takes less than five minutes, which offers the possibility of sensitivity analyses, e.g., of coolant mass flow rate. The results presented within this paper are compared with cooling experiments under laminar flow and a computational fluid dynamics solution of one trajectory point for the second Sharp-Edge Flight Experiment trajectory for turbulent flow. The values compare well with deviations of the wall temperature below 10% and deviations of heat flux below 18%. The investigation of coolant mass flow rates by means of HEATS show that for the entire second Sharp-Edge Flight Experiment trajectory the transpiration-cooling experiment should be run with 0.1 g/s $< \dot{m} <$ 1 g/s.

Nomenclature

A, B, C	=	at panels A, B, and C
a, b	=	Nusselt correlation coefficient
cond	=	conductive
c_f	=	friction coefficient
c_p	=	specific heat, J/kg · K
e	=	exhaust
F	=	film
g_*	=	solution of Crocco's equation
HG	=	hot gas
h	=	specific enthalpy, J/kg
i	=	in
K	=	von Kármán constant
l	=	length, m
l	=	laminar
Ma	=	Mach number
$\dot{m}$	=	mass flow rate, kg/s
mat	=	material
o	=	out
Pr	=	Prandtl number
p	=	pressure, Pa
$\dot{q}$	=	heat flux, W/m^2
Re	=	Reynolds number
r	=	recovery factor
rad	=	radiative
St	=	Stanton number
s	=	Reynold's analogy factor
T	=	temperature, K
t	=	time, s
t	=	turbulent
u	=	velocity, m/s
W	=	wall
x, y	=	coordinates
α_A	=	heat transfer coefficient, W/m^2 · K
α_V	=	volumetric heat transfer coefficient, W/m^3 · K
δ	=	film thickness, m
ϵ	=	emission coefficient
ϵ'	=	open porosity
η	=	efficiency
θ	=	deflection angle, °
κ	=	isentropic coefficient
λ	=	thermal conductivity, W/m · K
μ	=	dynamic viscosity, Pa · s
ρ	=	density, kg/m^3
σ	=	Stefan–Boltzmann constant
τ	=	shear stress, Pa
∞	=	ambient
$*$	=	normalized parameter

Presented at the 16th AIAA/DLR/DGLR International Space Planes and Hypersonic Systems and Technologies Conference, Bremen, Germany, 20–22 October 2009; received 14 September 2009; revision received 24 January 2010; accepted for publication 13 February 2010.

*Research Engineer, Institute of Structures and Design, Pfaffenwaldring 38-40; hannah.boehrk@dlr.de.

†Student, Institute of Structures and Design, Pfaffenwaldring 38-40.

I. Introduction

MANY applications are confronted with the necessity to estimate the heat flux from a fluid flow to a surface [1–4]. Especially when the surface is actively cooled, the determination of the heat transfer coefficient is difficult to assess [5]. Among other methods, active cooling can be film cooling, in which a layer of coolant blocks off the heat of a surrounding hot gas from the surface, or transpiration cooling, in which a surface is protected by coolant ejection through a permeable wall structure. The structure is cooled by both convection as the coolant passes through the pores and by the coolant wall flow, i.e., film, on the hot-gas side.

The engineering problem of the present paper is the determination of heat flux and wall temperature along the entire trajectory of the reentry vehicle SHEFEX II (Sharp-Edge Flight Experiment) [6–8]. On this reentry test bed, the flight experiment AKTiV (Aktive Kühlung im Versuch: active cooling experiment) investigating the influence of transpiration cooling using advanced permeable ceramic matrix composite material is foreseen [9,10]. This is of particular interest because novel permeable materials allow for new transpiration- or film-cooled heat-shield concepts. To lay out the transpiration element in terms of material thickness and coolant mass flow rate, a method is needed to calculate heat flux to the experiment in the uncooled, transpiration-cooled, and film-cooled regions. Moreover, this calculation is required for the entire trajectory in order to cover the different flight regimes and both laminar and turbulent flow.

This paper presents such a tool called HEATS. It uses a heat balance between hot flow, permeable material, and coolant flow and is based on known models of Crocco [2], Van Driest [3,4], and

Goldstein [11] in combination with the recent approach of Glass et al. [5]. At the expense of using empirical models, the calculation duration for the entire trajectory is less than 5 min. The advantage of this new tool is that the different conditions, (i.e., aerodynamic heating, and film and transpiration cooling) can be investigated separately. To prove the concept, results are compared with plasma wind-tunnel experiments for the laminar flow [12]. For turbulent flow they are compared with computational fluid dynamics (CFD) calculation.[‡] However, a CFD reference is only available for one trajectory point.

The next section introduces the trajectory with the parameters needed as input to the new heat balance method. Then laminar flow under pure aerodynamic heating is treated. The basic equations are presented and first results are compared with plasma wind-tunnel experiments. An extension to turbulent flows is outlined and a comparison with a CFD solution is shown. Exemplary HEATS results of the SHEFEX II trajectory for different materials are included. Finally, the implementation of film and transpiration cooling is described and wall temperature predictions for various amounts of coolant mass flow rates are given. Sensitivity to initial temperature and mass flow rate is shown. A summary concludes the main results that HEATS is a tool to lay out experiments, which include mass injection. Exemplarily, a prediction of the coolant mass flow for SHEFEX II is given.

II. Mission Outline

In the present case, the reentry vehicle SHEFEX II is investigated. The vehicle concept is depicted in Fig. 1. It consists of only flat and sharp-edged surfaces, providing similarity to the theoretical case of a flat plate. The interesting transpiration element, a porous and permeable C/C ceramic embedded in a C/C-SiC panel, is located on a panel of row C. The coolant is gaseous nitrogen. The down leg of the corresponding trajectory is presented in Fig. 2, starting from 100 km altitude, which corresponds to 641 s. Analytical equations for the oblique shock and expansion fans are used to determine the state variables outside the boundary layer of the vehicle surface. Figure 3 illustrates the approach exemplarily for panels A and B of SHEFEX II. This approach was demonstrated in a former investigation and validated by comparison with the CFD data of a particular available trajectory point [9].

Figure 2 shows the state variable's pressure and temperature at panels B and C during the SHEFEX II reentry. It can be seen that the temperature peak occurs earlier than the pressure peak. When the temperature delay due to the capacity of the thermal structure is considered, peak temperature inside the heat-shield material and maximum surface pressure will be reached at nearly the same time [13]. These state variables of the atmospheric gas aerodynamically heating the surface are used as input data to HEATS.

III. Concept of HEATS

HEATS is a computer program intended for the layout of transpiration cooling and therefore assesses wall temperatures to a surface at transpiration-cooled, film-cooled, or uncooled condition. The problem is approached in three steps, sketched in Fig. 4. Step 1 includes the heat flux to the panels as in a parallel plate case. The heat balance for the surface in this case equals

$$\dot{q}_{\mathrm{HG}-W} = \dot{q}_{\mathrm{rad}} + \dot{q}_{\mathrm{cond}} \tag{1}$$

with index $\mathrm{HG}-W$ indicating heat transfer from the hot gas to the wall.

Step 2, addressed in region 2 of Fig. 4, additionally takes into account the thermal blocking by a coolant layer (film cooling), which is injected through the porous material C/C in the case of the experiment presented here. The heat balance for the surface remains

[‡]Private communication with T. Barth, DLR, German Aerospace Center, November 2008.

Fig. 1 SHEFEX II reentry vehicle.

$$\dot{q}_{F-W} = \dot{q}_{\mathrm{rad}} + \dot{q}_{\mathrm{cond}} \tag{2}$$

with index $F-W$ for heat transfer from film to the wall and the heat balance for the cooling film is expressed as

$$(\dot{q}_{\mathrm{HG}-F} - \dot{q}_{F-W})\Delta l = (h_{F,o}\rho_{F,o}u_{F,o} - h_{F,i}\rho_{F,i}u_{F,i})\delta_F \tag{3}$$

with control volume length Δl and film thickness δ_F assumed as constant. The heat balance of Eq. (3) is an energy balance of a stationary flow when the effect of work is neglected and potential and kinetic energy are constant. No mixing between the hot gas and the film is taken into account in laminar case. The case for turbulent flow is discussed in detail in Secs. III.A.2–III.C.2.

Step 3 addresses all three effects, heat flux from the hot gas to the film $\dot{q}_{\mathrm{HG}-F}$, from the film to the wall $\dot{q}_{F-W}$, and heat transfer from the hot wall to the transpired coolant as the coolant temperature increases. The respective heat balance is summarized in Sec. III.C.

The present paper subsequently explains how these equations were considered and which models have been applied for both laminar and turbulent flow condition, then were implemented and solved. comparison with detailed numerical CFD calculations or to experiments is shown within the respective chapter, taking into account the boundary conditions of the respective comparison case.

A. Aerodynamic Heating (Region 1)

This section treats region 1, where the wall is aerodynamically heated. The thermal energy

$$\dot{q}_{\mathrm{HG}-W} = \alpha_A(T_r - T_W) \tag{4}$$

is transferred from the hot gas to the wall through convection with the convection heat transfer coefficient α_A and the recovery temperature T_r. These parameters are functions of the flow properties and can be expressed as

$$\alpha_A = St\rho_\infty c_{p,\infty}u_\infty \tag{5}$$

and

$$T_r = T_\infty\left(1 + r\frac{\kappa-1}{2}Ma_\infty^2\right) \tag{6}$$

The two commonly unknown variables of Eqs. (5) and (6) are the Stanton number St and the recovery factor r. They must be determined for each flow condition, be it laminar or turbulent.

To solve the heat balance problem of Eq. (1), radiation heat flux is determined to

$$\dot{q}_{\mathrm{rad}} = \sigma\epsilon T^4 \tag{7}$$

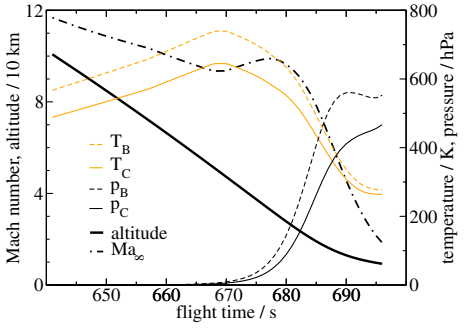

Fig. 2 Pressure and gas temperature outside the boundary layer of panels B and C during reentry flight.

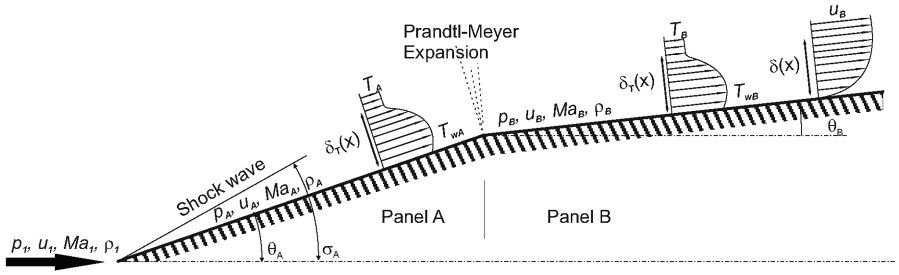

Fig. 3 SHEFEX II shock and expansion areas.

with Stefan-Boltzmann-constant σ and the wall material's emissivity ϵ.

In a radiation adiabatic case, the third term of Eq. (1), the heat flux due to conduction $\dot{q}_{\text{cond}}$ within the material equals zero. However, for the transient determination of the heat flux, the heat equation

$$\rho_{\text{mat}} c_{p,\text{mat}} \frac{\partial T}{\partial t} = \lambda_y \frac{\partial^2 T}{\partial y^2} + \lambda_x \frac{\partial^2 T}{\partial x^2} \tag{8}$$

is used with a boundary condition for the surface of third order with

$$\dot{q}_{\text{cond}} = \lambda_y \left(\frac{\partial T}{\partial y} \right)_W \tag{9}$$

and a boundary condition of second order at the rear side and the edges of

$$\lambda_y \left(\frac{\partial T}{\partial y} \right)_W = 0 \tag{10}$$

i.e., assuming that these sides are adiabatic. Table 1 gives the characteristic values for the heat-shield materials C/C of the permeable and porous probe and C/C-SiC of the TPS panels. Note that the panel has to be treated as orthotropic material. Both are used in the transpiration element of SHEFEX II and their values are used for the present calculation with HEATS. They are assumed here as constant over temperature.

In HEATS, Eq. (8) is solved using an explicit finite difference method. The panel is discretized into a grid of $n_x \times n_y$ points spaced by a distance Δx and Δy, respectively, parallel and perpendicular to the flow, as sketched in Fig. 5. Then, using a forward difference at the time t and a second-order central difference for the space differentiation at positions x and y, the discretized Fourier's law [14]

$$\begin{aligned} \rho_{\text{mat}} c_{p,\text{mat}} \frac{T^{t+\Delta t}(x,y) - T^t(x,y)}{\Delta t} &= \frac{\lambda_x}{\Delta x^2} [T^t(x+\Delta x, y) - 2T^t(x,y) \\ &+ T^t(x-\Delta x, y)] + \frac{\lambda_y}{\Delta y^2} [T^t(x, y+\Delta y) - 2T^t(x,y) \\ &+ T^t(x, y-\Delta y)] \end{aligned} \tag{11}$$

is obtained with boundary conditions

$$\dot{q}_{\text{cond}} = \frac{\lambda_y}{\Delta y} [T^t(x,0) - T^t(x,\Delta y)] \tag{12}$$

for the surface in contact with the hot flow and

$$T^t(0,y) = T^t(\Delta x, y) \tag{13}$$

$$T^t(x, n_y \times \Delta y) = T^t(x, (n_y - 1) \times \Delta y) \tag{14}$$

and

$$T^t(n_x, y) = T^t((n_x - 1) \times \Delta x, y) \tag{15}$$

for the adiabatic surface.

As commonly known, the value of Δt has to be chosen, knowing that the smaller Δt, the more precise the results but the more time-consuming the calculation. To guarantee the stability of the scheme, Δt has to respect the so-called Courant–Friedrichs–Lewy conditions [14]:

$$\Delta t \leq \frac{\Delta x^2}{2 \frac{\lambda_x}{\rho_{\text{mat}} c_{p,\text{mat}}}} \quad \text{and} \quad \Delta t \leq \frac{\Delta y^2}{2 \frac{\lambda_y}{\rho_{\text{mat}} c_{p,\text{mat}}}} \tag{16}$$

To implement this method, an initial panel temperature must be given and has a certain influence on the results. This temperature is known in the case of a ground test, but is difficult to determine in the case of a reentry. In the present case 200 K are assumed, and a sensitivity analysis will show how this temperature affects the wall temperature in the hot phase of the reentry.

The presented method provides the possibility to quickly calculate the heat flux to a flat plate in the case of parallel flow. The heat flux to the wall can now be determined for flow over a flat plate, depending on the temperature in the undisturbed vicinity. The first step and its implementation will be verified in the next paragraph by comparison with experiments and numerical data for both laminar and turbulent flow, respectively.

1. *Laminar Flow*

The heat flux to the panels is determined from the state variables of the hot gas at the boundary-layer edge of the surface, as mentioned above. It is determined for the laminar case by means of Crocco's method, in which a thin boundary layer on a flat plate is considered without pressure gradient, i.e., $\partial p/\partial y = \partial p/\partial x = 0$. The motion is assumed as two-dimensional and steady state, and mixing of the hot gas and the coolant is neglected. According to Van Driest [3], Crocco's method is based on the three major equations:

$$\tau = \mu \frac{\partial u}{\partial y} \tag{17}$$

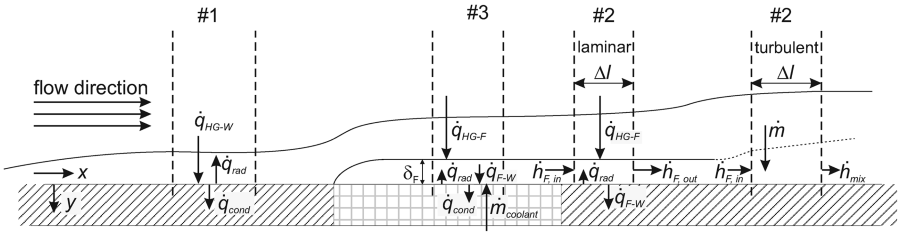

Fig. 4 HEATS heat balance concept.

Table 1 Material values of C/C and C/C-SiC

	ρ, kg/m	ϵ	λ_x/W/m K, W/mK	λ_y, W/mK	c_pJ/kgK	k_D, m^2	k_F, m	a [21]	b [21]
C/C	1400	0.88	14×10^{-6}	2×10^{-6}	1650	1.645×10^{-13}	2.9×10^{-6}	2.22×10^{-6}	0.703
C/C-SiC	1900	0.88	17×10^{-6}	8.4×10^{-6}	1350	——	——	——	——

$$g_* g_*'' + 2u_* \rho_* \mu_* = 0 \tag{18}$$

and

$$\left(h_*'' + Pr\frac{u_\infty^2}{h_\infty}\right) g_* + (1 - Pr) h_*' g_*' = 0 \tag{19}$$

These relations are derived from the conservation equations of mass, momentum, and energy in the boundary layer using the Newtonian shear stress under the boundary conditions

$$g_*' = 0, \qquad h_* = h_W/h_\infty \quad \text{at } u_* = 0 \tag{20}$$

and

$$g_* = 0, \qquad h_* = 1 \quad \text{at } u_* = 1 \tag{21}$$

for constant Prandtl number Pr, enthalpy h, velocity u, and

$$g_* = (4x\tau/\rho_\infty \mu_\infty u_\infty^3) \tag{22}$$

The subscript ∞ relates to the variables in the undisturbed flowfield. The subscript $*$ indicates variables made dimensionless with respect to the undisturbed flowfield, e.g., $u_* = u/u_\infty$.

The enthalpy distribution according to Eq. (19) is calculated using the Blasius distribution of the dimensionless shear function as given in Van Driest [3].

Writing Eq. (18) in integral form and taking into account the boundary conditions of Eq. (20), substitution, integration, re-substitution, and reintegration yield

$$g_*(u_*) = g_*(1-c) + (1-u_*)\int_0^{u_*} \frac{f(u_*)}{g_*(u_*)}\,\mathrm{d}u_* - c\int_0^{1-c} \frac{f(u_*)}{g_*(u_*)}\,\mathrm{d}u_* + \int_{u_*}^{1-c} (1-u_*)\frac{f(u_*)}{g_*(u_*)}\,\mathrm{d}u_* \tag{23}$$

with $f(u_*) = 2u_*\rho_*\mu_*$ and c as an arbitrarily small value greater than zero. To now determine an appropriate solution for $g_*(1-c)$ in concurrence with the boundary condition $g_*(1) = 0$, Crocco derived the combination [2]

$$\frac{\bar{\bar{g}}(1-c) - c}{c|\bar{\bar{g}}'(1-c)|} = 0.7828 + 0.0178|\bar{\bar{g}}'(1-c)| \tag{24}$$

with $g_*(1-c) = \bar{\bar{g}}(1-c) + \delta g_*$. It is found in Van Driest [3] that the term δg_* is negligible, since on the order of 10^{-4}.

After solution of g_*, the local skin-friction coefficient c_f of the smooth surface is determined with the local Reynolds number Re_x at flow position x to

$$c_f = \frac{g_*(0)}{\sqrt{Re_x}} \tag{25}$$

providing the surface stress $\tau_{\mathrm{HG}-W}$

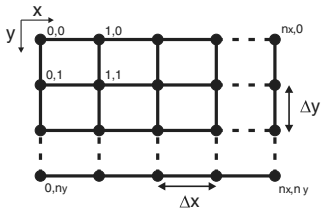

Fig. 5 Discretization of the panel.

Table 2 Inflow condition of plasma wind-tunnel experiments

Condition	L2K	L3K FCIII	L3K FCIII
Ma	7.0	7.5	7.5
p_{stat}, Pa	47	56	56
T_{stat}, K	378	530	530
Deflection angle θ, °	20	20	30
L, mm	295	222	222

$$\tau_{\mathrm{HG}-W} = \tfrac{1}{2} c_f \rho_\infty u_\infty^2 \tag{26}$$

The Stanton number for solution of Eq. (5) yields

$$St = \frac{c_f}{2Pr^{2/3}} \tag{27}$$

and the recovery factor for Eq. (6) is determined with

$$r = \sqrt{Pr} \tag{28}$$

for laminar boundary layers [3]. The heat flux to the wall can now be determined for laminar flow over a flat plate in dependence of the flow temperature, velocity and species in the undisturbed vicinity.

The determination of the laminar heat flux by HEATS is used here in order to compare the heat balance strategy to three experiments that were conducted in the DLR wind tunnels L2K and L3K during the RESPACE and IMENS$^+$ test campaigns [12]. The setup, a wedge model with a front leading edge with a radius of 13 mm, was inclined by a deflection angle of θ with the porous probe located in the center of the setup [12]. The inflow conditions of the plasma wind-tunnel flow are listed in Table 2, resulting in Reynolds numbers on the order of $Re \approx 10^4$, indicating that the flow is laminar. Figure 6 shows the temperature traces of the L2K and L3K conditions at aerodynamic heating of the C/C-SiC surface just upstream the porous probe. The stagnation point on the model is chosen as the origin of body coordinate x.

At the measurement point, the boundary-layer thickness is on the order of the shock standoff distance so that the entropy layer that has risen from the curved shock in front of the wedge model is swallowed [10,15]. The flow can thus be considered as homentropic and all calculation rules introduced above apply to the present flow region. The dashed lines give the surface temperature at the same position determined by HEATS. For these calculations, the specific heat c_p and the isentropic coefficient κ of the hot gas are derived from the equilibrium model LibIdGasMix from FluidMAT (Hochschule

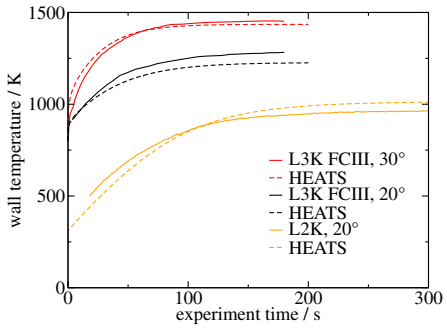

Fig. 6 HEATS data validated with the measured surface temperature at $\theta = 20°$ in L2K and $\theta = 20$ and 30° in L3K for a C/C-SiC surface. Measurement data from RESPACE and IMENS$^+$ [12].

Zittau/Görlitz—University of Applied Sciences). The dynamic viscosity, μ is determined by Sutherland's law and the Prandtl number was chosen as $Pr = 0.75$. It can be seen that the HEATS data compare well with the temperatures of the experiments.

2. *Turbulent Flow*

During the SHEFEX II reentry flight, the flight condition, as opposed to that in the plasma wind tunnel, will be turbulent. Turbulence leads to an increase of heat flux to the wall and modifies the convection heat transfer coefficient significantly [1]. Thus, the method as presented so far is not yet sufficient for the prediction of heat flux to an entire trajectory.

For turbulent heat transfer Van Driest's approach is followed, where both Stanton number and recovery factor are determined assuming that the shear stress distribution is linear with the distance from the wall [4]. Using von Kármán's method according to which the viscous subregion can be divided into the laminar and transitional layers, the recovery factor hence yields [4]

$$r = Pr_t\left[1 + \frac{2}{K}\sqrt{\frac{c_f}{2}}(1 - Pr_t)\left[\frac{\pi^2}{6} + \frac{3}{2}(1 - Pr_t)\right] + 25\frac{c_f}{2}\left\{\left(\frac{Pr_l}{Pr_t} - 1\right) + 2\,\ell_n\left[1 + \frac{5}{6}\left(\frac{Pr_l}{Pr_t} - 1\right)\right] + \ell_n 6 \cdot \ell_n\left[1 + \frac{7}{8}\left(\frac{Pr_l}{Pr_t} - 1\right)\right] - \ell_n 6 \cdot \ell_n\left[1 + \frac{1}{4}\left(\frac{Pr_l}{Pr_t} - 1\right)\right]\right\}\right] \tag{29}$$

where von Kármán's constant $K = 0.4$ and Pr_t is the turbulent Prandtl number, which is assumed as 0.85 [4]. The Stanton number is expressed as a function of the Reynolds analogy factor s and the friction coefficient as in

$$St = \frac{1}{s}\frac{c_f}{2} \tag{30}$$

The Reynolds analogy factor and the friction coefficient are in turn computed by [4]

$$s = Pr_t\left[1 + \left\{\frac{(1 - Pr_t)}{5K}\left[\frac{\pi^2}{6} + \frac{3}{2}(1 - Pr_t)\right] + \left(\frac{Pr_l}{Pr_t} - 1\right) + \ell_n\left[1 + \frac{5}{6}\left(\frac{Pr_l}{Pr_t} - 1\right)\right]\right\}5\sqrt{\frac{c_f}{2}}\right] \tag{31}$$

and

$$\frac{0.242}{\sqrt{c_f\left(\frac{\kappa-1}{2}Ma_\infty^2\right)}}(\sin^{-1}\alpha + \sin^{-1}\beta) = 0.41 + \log_{10}(Re_x c_f) - f(n)\log_{10}\left(\frac{T_W}{T_\infty}\right) \tag{32}$$

with

$$\alpha = (2A^2 + B)(B^2 + 4A^2)^{-\frac{1}{2}} \tag{33}$$

$$\beta = B(B^2 + 4A^2)^{-\frac{1}{2}} \tag{34}$$

$$A^2 = \frac{\kappa - 1}{2}Ma_\infty^2\left(\frac{T_\infty}{T_W}\right) \tag{35}$$

and

$$B = \left(1 + \frac{\kappa - 1}{2}Ma_\infty^2\right)\left(\frac{T_\infty}{T_W}\right) - 1 \tag{36}$$

and a function $f(n)$ equal to 0.5 for air at high temperature. At Reynolds numbers of $3 \times 10^5 < Re < 3 \times 10^6$, the Stanton number and recovery factor are determined as half-turbulent and half-laminar numbers. All gas properties of the nitrogen coolant and the hot air are taken from FluidMAT.

Figure 7 gives the wall temperatures of the critical point of the reentry trajectory solved with computational fluid dynamics (see footnote ‡) with the numerical code TAU. The CFD results are considered a reference, since TAU has been proven to reliably determine wall temperatures in comparable conditions in the past [16–18]. The conditions are $h = 20$ km, $Ma = 8$, angle of attack of 2.5°, and a turbulent boundary layer at radiation adiabatic condition. The emissivity used for this simulation was 0.85 and that in HEATS was adapted to this case. To be able to neglect the influence of the angle of attack, the temperature values at the panel row of the side of the vehicle is chosen for comparison with HEATS.

The HEATS data for radiation adiabatic wall temperature are also given in Fig. 7. These data can be determined by HEATS by setting thermal conductivity and heat capacity of the wall to zero. The tip of the vehicle's sharp nose is chosen as the origin of body coordinate x so that the incoming boundary layer is treated as continuous from tip to the point of interest. The data compares well with the CFD results, with a deviation of less than 5% for panels A, B, and C. Figure 7 shows also the C/C-SiC transient wall temperature for turbulent heat flux to panel rows A, B, and C. The assessed temperatures at panel C are higher by 58% in the radiation adiabatic case and the comparison of the curves of the radiation adiabatic and transient case shows the temperature delay and supports the earlier statement that maximum heat load and maximum pressure are encountered approximately at the same time.

For aerodynamic heating of the porous C/C probe, it can be seen in Fig. 8 that due to lower thermal conductivity, the wall temperature rises more steeply and to higher temperatures than with C/C-SiC. For comparison, an exemplary wall temperature is given for heat flux to the C/C probe at panel C, assuming that the surrounding flow was laminar. The figure shows also that when turbulence is ignored, heat load for the trajectory of SHEFEX II is underestimated by 55% in transient condition and 28% in radiation adiabatic condition. From the turbulent conditions with $Re > 3 \times 10^6$, it is found that along the trajectory, turbulent flow is encountered from an altitude of ~35 km, i.e., from $t = 677.5$ s.

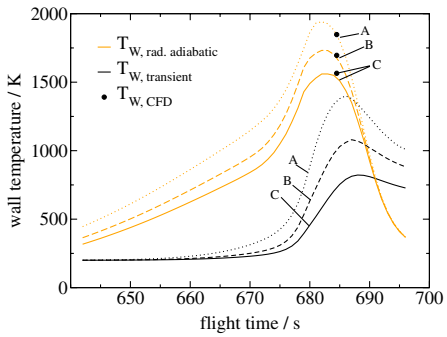

Fig. 7 Radiation adiabatic and transient wall temperature from HEATS and CFD (see footnote ‡).

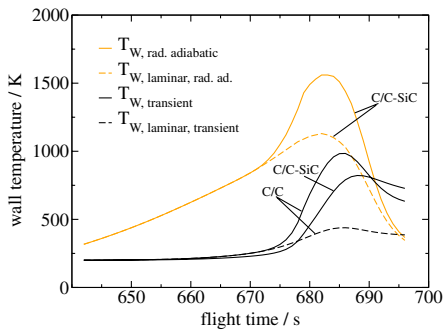

Fig. 8 Wall temperature at panel C from HEATS.

B. Wall Heat Flux During Film Cooling (Region 2)

It was shown above that HEATS is able to determine the transient wall temperature of a wall exposed to turbulent hypersonic flow, taking into account the wall heat conduction. In film cooling, the structure is covered by a coolant layer on the outer hot surface. The layer reduces the heat transfer from the high-enthalpy environment to the vehicle surface. Moreover, a coolant film (for example, of nitrogen) may also provide oxidation protection for the structure, which may be an important issue in case of carbon-based material.

In HEATS, the film is treated as a layer, the heat transfer toward which is determined by the methods described above. In the laminar case, no admix of the surrounding hot atmospheric gas is assumed, and the heat transfer for both hot-gas-to-film and film-to-wall are determined by Crocco's model. Under turbulent conditions, the Van Driest approach is used for both. As a first approach the velocity of the film is set to $u_F = 0.1 \times u_\infty$ and the temperature of the film outside the boundary layer is determined, for example, by calculation of the heat exchange during transpiration as will be explained in Sec. III.C.

1. *Laminar Flow*

Comparison of HEATS results with the same experiment campaign mentioned in Sec. III.A.1 proves that the model applied here, with the two heat balances hot-gas-to-film and film-to-body, is a valid one. Since the hot-gas flow is laminar, no mixing of the hot gas and the film is assumed. The film thickness δ_F is assumed as constant and considered as a pure heat-flux-blocking layer between wall and vicinity. Equation (3) gives the heat balance that applies for this case.

As shown in Fig. 9, the cooling of the wall can be predicted with the input parameters of Table 1, an initial temperature of 293 K, a reservoir gas temperature of 422 K, a Prandtl number of 0.75, and the geometric values of the wedge model. The figure shows that accurate data are predicted under laminar conditions.

2. *Turbulent Flow*

Turbulent flow is characterized by a strong vorticity, leading to a mix between the two gas flows, hot and film, and reducing the cooling efficiency. In the heat balance of the coolant film as in Eq. (3), the term of convection between hot-gas flow and film is replaced by a term accounting for the entraining hot-gas mass into the film and the subsequent heat adjustment between the fluids. Equation (3) becomes

$$\dot{m} c_{p,\infty} T_\infty - \dot{q}_{F-W} \Delta l = -(c_p T \rho u)_{F,i} \delta_{F,i} + ((\rho u)_{F,i} \delta_{F,i} + \dot{m}) c_{p,\mathrm{mix}} T_{\mathrm{mix}} \tag{37}$$

with growing film thickness δ_F. The factor $\dot{m}$ describes the mass of air entering into the film. It is computed using Goldstein's theory, according to which the entering amount of air is proportional to that forming a boundary layer, which begins to rise from the rear edge of the porous material without cooling [11]. The coolant mass flow rate can be integrated according to

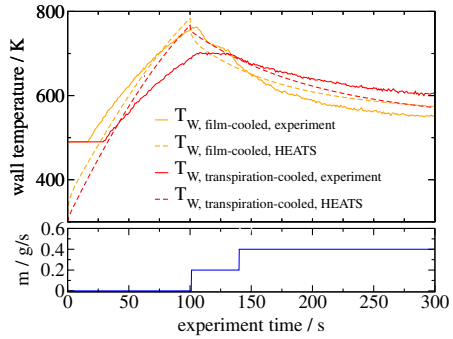

Fig. 9 HEATS data validated with plasma wind-tunnel data measured during nitrogen mass flow of 0.4 g/s at $\theta = 20°$ in L2K for a C/C-standard probe. Measurement data from RESPACE and IMENS$^+$ [12].

$$\dot{m} = \rho_\infty \int_0^\delta u(y)\, \mathrm{d}y \tag{38}$$

which, with the one-seventh-velocity-profile [19], results in [20]

$$\dot{m}(x) = \tfrac{7}{8} \rho_\infty u_\infty \delta(x) \tag{39}$$

where

$$\delta = 0.376 x Re_x^{-0.2} \tag{40}$$

All flow properties of the gas mix are determined by interpolation according to the mass ratio of the mixing flows.

C. Wall Heat Flux During Transpiration Cooling (Region 3)

Finally, region 3 will be addressed, in which the heat exchange between the structure and the transpiring coolant is determined. The mean exhaust velocity u_e of the cooling gas is with [21]

$$u_e = \frac{u_{\mathrm{filter}}}{\epsilon'} \tag{41}$$

proportional to the filter velocity of the gas through the porous volume determined by [22]

$$\frac{\partial p}{\partial y} = \frac{p^2 - p_\infty^2}{2 p_\infty d_s} = \frac{\mu}{k_D} u_{\mathrm{filter}} + \frac{\rho}{k_F} u_{\mathrm{filter}} \tag{42}$$

The values of Darcy coefficient k_D and Forchheimer coefficient k_F are listed in Table 1.

The exhausted coolant flow must not trigger or intensify turbulence and subsequently intensify the heat flux to the wall. An attempt is made to judge whether or not this takes place by means of the blowing ratio:

$$F = \frac{\rho_e u_e}{\rho_\infty u_\infty} \tag{43}$$

For one inflow condition the triggering of turbulence was identified by Heufer [19] and Heufer and Olivier [23] to be greater than 0.144. Taking this value obtained from coolant ejection through a slit as a criterion for transpiration cooling is, however, a conservative approach.

The cooling of the inner structure of the porous material is carried out by convective heat transfer between the material and the coolant. Radiation within the porous structure is neglected. According to Glass et al. [5], the balance for the wall material is

$$\lambda_x \frac{\partial^2 T_{\mathrm{mat}}}{\partial x^2} + \lambda_y \frac{\partial^2 T_{\mathrm{mat}}}{\partial y^2} - \alpha_V (T_{\mathrm{mat}} - T_F) = \rho_{\mathrm{mat}} c_{p,\mathrm{mat}} \frac{\partial T_{\mathrm{mat}}}{\partial t} \tag{44}$$

and the one for the gas, accordingly, is

$$-\frac{\partial (\frac{\dot{m}(x,y)}{A} c_{p,F} T_F)}{\partial x} - \frac{\partial (\frac{\dot{m}(x,y)}{A} c_{p,F} T_F)}{\partial y} - \alpha_V (T_{\mathrm{mat}} - T_F) = \rho_F c_{pF} \frac{\partial T_F}{\partial t} \tag{45}$$

Only the pressure gradient in flow direction is taken into account, so that

$$-\frac{\dot{m}}{A} \frac{\partial (c_{p,F} T_F)}{\partial y} - \alpha_V (T_{\mathrm{mat}} - T_F) = \rho_F c_{pF} \frac{\partial T_F}{\partial t} \tag{46}$$

The volumetric heat transfer coefficient α_V is determined by the Nusselt correlation [21],

$$\alpha_V = Nu \lambda / k_D = a (Re)^b \lambda / k_D \tag{47}$$

with the Reynolds number of the exhausted coolant [5]:

$$Re = \rho_F \frac{k_D^{1.5}}{\mu \epsilon'} \frac{\Delta p}{\Delta y} \tag{48}$$

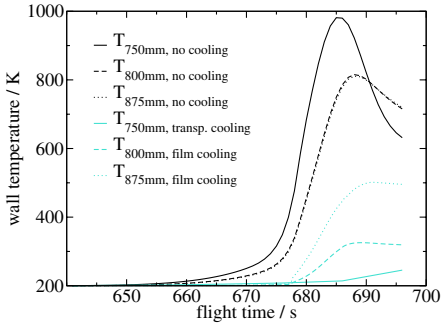

Fig. 10 Wall temperature of SHEFEX II without and with transpiration and film cooling.

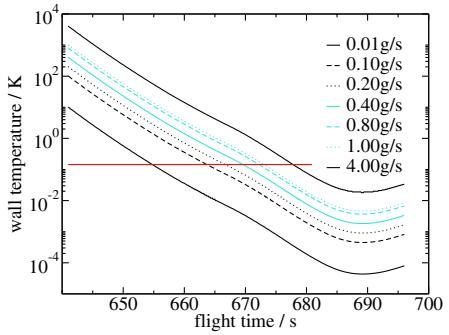

Fig. 13 Blow rates during SHEFEX II reentry for various mass flow rates.

The coefficients a and b are listed in Table 1 [21]. As boundary conditions, it is assumed that the rear of the panel is adiabatic and that the coolant there has the same temperature as that in the reservoir, i.e., 300 K.

1. *Laminar Flow*

Figure 9 shows the results of the transpiration-cooling experiment conducted within RESPACE and IMENS$^+$. According to the coolant mass flow rate given in the bottom of the diagram, the wall temperatures at the position of aerodynamic heating and transpiration and film cooling are measured by an infrared camera.

Figure 9 shows in solid graphs the measurement data of the region where nitrogen is transpired for cooling, and in dashed graphs the time-resolved wall temperature determined by HEATS. Comparison with the film-cooled curves shows that the transpiration cooling results in lower wall temperature by a few percent. The curves show that the HEATS data agree well with the measurement data, with a deviation below 10%.

2. *Turbulent Flow*

The temperature of the transpiration-cooling experiment on SHEFEX II at position 750 mm downstream of the SHEFEX II tip is given in Fig. 10 for the reentry trajectory. The film-cooled wall temperatures at 800 and 875 mm are shown. These positions correspond to the center of the porous and permeable C/C probe and two downstream positions with heat-shield material C/C-SiC, where only film cooling is active. Transient heat flux is calculated.

In the turbulent flow regime, in comparison with the laminar condition, the coolant film is significantly intruded by the hot atmospheric gas. Because of the exhausted coolant at a provided specific impulse, however, the high-enthalpic gas of the atmosphere is expected not to come in contact with the vehicle wall, despite the present turbulence. Transpiration cooling relative to film cooling is thus of larger importance in the turbulent flow regime, where the film may be purged by the intruding hot air.

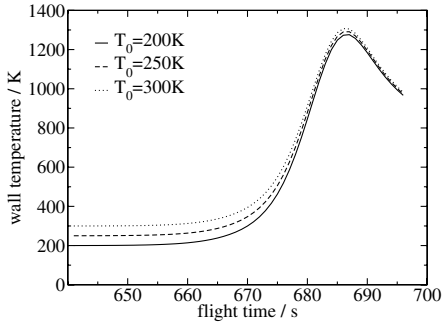

Fig. 11 Transient wall temperatures at panel B for varying initial panel temperature.

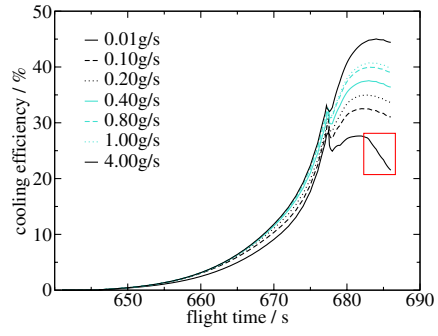

Fig. 12 Cooling efficiency for various mass flow rates.

IV. Conclusions for SHEFEX II

SHEFEX II, an experimental reentry vehicle, carries a transpiration- and film-cooling experiment. The present paper has presented the method of determination and prediction of the transient wall-cooling effects by transpiration of a film through a permeable ceramic matrix composite structure during the SHEFEX II reentry trajectory.

For the transient heat flux to the structure, an initial temperature of the material of 200 K is assumed at an altitude of 100 km. Figure 11 shows the influence of the initial temperature on the transient wall temperature trajectory. It can be seen that at high altitude, the wall is neither cooled nor heated and thus remains nearly constant. When approaching the temperature peak of the trajectory at lower altitudes and denser atmospheric air, however, the wall temperatures are mostly adjusted to a deviation of less than 10% from each other at 679 s. At peak heating, i.e., time point 687 s, the deviation is below 3%. This shows that in the case of a reentry without cooling, the initial temperature is no critical parameter but has negligible impact on the maximum thermal load applied on the panels.

Experiments had been conducted in a plasma wind tunnel in former campaigns, however, under laminar flow condition. By means of HEATS, the mass flow rate that must be used under the turbulent flow conditions to which SHEFEX II is to be exposed shall now be isolated.

Figure 12 shows for the position 875 mm, i.e., in the film-cooling region downstream of the C/C probe, the cooling efficiency is defined by

$$\eta = 1 - \frac{T_{\text{cooled}}}{T_{\text{uncooled}}} \tag{49}$$

The small peak on the rising flank of the curves origins from a calculatory discontinuity. When the calculation method changes from laminar to turbulent at $Re = 1.6 \times 10^6$, the flow properties are henceforth determined as those of the gas mix by interpolation as mentioned above. For a mass flow rate as small as 0.01 g/s, it can be seen in the diagram that the film is purged by the turbulent boundary layer, resulting in a steep decrease of the cooling efficiency η. It is concluded that the mass flow rate used for the cooling of the ceramic matrix composite heat shield should be chosen to $\dot{m} \geq 0.1$ g/s.

In Fig. 13, the blow rates of each of the mass flow rates are plotted. A line indicates the reference of $F = 0.144$ that was chosen as upper limit [19]. At very low atmospheric density, the blowing forms a jet. From a trajectory point fairly before the rising of the wall temperature due to increasing atmospheric density, the blowing should switch to a wall flow in order to provide the efficiency determined in Fig. 12. This time point $t = 675$ s, as can be seen in Fig. 7. From Figure 13, it is hence concluded that the mass flow rate must lie at $\dot{m} \leq 1$ g/s.

Consequently, the chosen mass flow rate for the transpiration-cooling experiment must be chosen to $0.1 \text{ g/s} \leq \dot{m} \leq 1$ g/s.

V. Conclusions

The present paper presents the layout tool HEATS for the determination of transient wall heat flux to a transpiration-cooled parallel wall under laminar or turbulent flow conditions. HEATS is based on a heat balance analysis using a heat balance between hot flow, permeable material, and coolant flow.

With this tool, a scientific investigation of transpiration cooling for various high temperature applications becomes feasible. The method is used here to determine the transient heat flux to SHEFEX II. Transient wall temperature determination has been validated for both C/C and C/C-SiC by comparison with experiments of the RESPACE and IMENS$^+$ test campaigns. Moreover, turbulent wall temperature was compared with a CFD solution of the critical point of the reentry path and it is shown that with HEATS, a good prediction of the heat-shield panel temperatures during aerodynamic heating is possible. The results of the CFD solution and HEATS compare well with, respectively, deviations of the wall temperature below 10% and deviations of heat flux below 18% from the reference value. However, the CFD solution results from radiation adiabatic assumption and HEATS had to be adapted to this flow case.

From a sensitivity analysis the necessary mass flow rate for the SHEFEX II transpiration element is determined to $0.1 \text{ g/s} < \dot{m} < 1$ g/s. This results from a consideration of the entire reentry trajectory. The lower and upper limitations result, respectively, from purging of the film at too low of a mass flow and from lifting of the wall jet at too high of a mass flow rate. The calculation duration of which for the 45 s reentry is short with less than 5 min.

Future investigations have to focus on a more detailed analysis of the velocity of the film parallel to the wall, because it is of influence to cooling efficiency. For the present investigation, this velocity was assumed to be 10% of the hot-gas velocity outside the vehicle and good results are achieved.

Moreover, due to the straightforward approach with considerably high theoretical details under short calculation times, HEATS is predestined for solving heat transfer problems when a structure is actively cooled. These are, for example, effusion cooling of a combustion chamber wall or the investigation of scaling laws for downscaled transpiration-cooling wind-tunnel models.

References

[1] Anderson, J. D., *Hypersonic and High Temperature Gas Dynamics*, McGraw–Hill, New York, 1989.

[2] Crocco, L., "Transmission of Heat from a Flat Plate to a Fluid Flowing at a High Velocity," NACA TM-690, Feb. 1932.

[3] Van Driest, E. R., "Investigation of Laminar Boundary Layer in Compressible Fluids Using the Crocco Method," NACA TN-2597, 1952.

[4] Van Driest, E. R., "The Problem of Aerodynamic Heating," *Aeronautical Engineering Review*, Vol. 15, No. 10, Oct. 1956, pp. 26–41.

[5] Glass, D. E., Dilley, A. D., and Kelly, H. N., "Numerical Analysis of Convection/Transpiration Cooling," *Journal of Spacecraft and Rockets*, Vol. 38, 2001, pp. 15–20. doi:10.2514/2.3666

[6] Weihs, H., Longo, J., Turner, J., "The Sharp Edge Flight Experiment SHEFEX II: A Mission Overview and Status," 15th International Space Planes and Hypersonic Systems and Technologies Conference, AIAA Paper 2008-2542, April 2008.

[7] Weihs, H., Longo, J., and Gülhan, A., "The Sharp Edge Flight Experiment SHEFEX," *4th European Workshop on Hot Structures and Thermal Protection Systems for Space Vehicles*, ESA, SP-521, Paris, Nov. 2002. pp. 53–56.

[8] Turner, J., Hörschgen, M., Jung, W., and Turner, P., "SHEFEX 2—The Vehicle, Subsystems and Mission Concept for a Hypersonic Re-Entry Flight Experiment," *18th ESA Symposium on European Rocket and Balloon Programmes and Related Research*, ESA SP-647, Paris, Nov. 2007.

[9] Böhrk, H., Kuhn, M., and Weihs, H., "Concept of the Transpiration Cooling Experiment on SHEFEX II," *2nd International ARA-Days*, Arcachon, France, Oct. 2007.

[10] Böhrk, H., Kuhn, M., and Weihs, H., "Concept of the Heat Balance of the Transpiration-Cooled Heat Shield Experiment AKTiV on SHEFEX II," *6th European Workshop on Thermal Protection Systems & Hot Structures*, Stuttgart, Germany, Apr. 2009.

[11] Goldstein, R. J., "Film Cooling," *Advances in Heat Transfer*, edited by T. F. Irvin and J. P. Hartnett, Academic Press, New York, 1971, pp. 321–379.

[12] Kuhn, M., and Hald, H., "Application of Transpiration Cooling for Hot Structures," *Notes on Numerical Fluid Mechanics and Multidisciplinary Design*, Vol. 98, edited by A. Gülhan, 2008, pp. 82–103.

[13] Reimer, T., and Laux, T., "Thermal and Mechanical Design of the Expert C/C-SiC Nose," *Proceedings of the 5th European Workshop on Thermal Protection Systems and Hot Structures*, SP-631 2006.

[14] Schwarz, H. R., and Köckler, N., *Numerische Mathematik*, Vol. 6, Teubner, Wiesbaden, Germany, 2006.

[15] Hirschel, E. H., and Zarchan, P., "Basics of Aerothermodynamics," *Progress in Astronautics and Aeronautics.*, Springer, New York, 2006.

[16] Barth, T., "Considerations on CFD Modeling for the Design of Re-Entry Vehicles: Aero- and Thermodynamic Analysis of SHEFEX I," *Engineering Applications of Computational Fluid Mechanics*, Vol. 2, No. 1, 2008, pp. 76–84.

[17] Martinez Schramm, J., Wagner, A., Wolfram, J., Hannemann, K., Barth, T., and Mulot, J.-D., "Post Flight Analysis of SHEFEX I: Shock Tunnel Testing and Related CFD Analysis," *16th AIAA/DLR/DGLR International Space Planes and Hypersonic Systems and Technologies Conference*, Bremen, Germany, 2009.

[18] Martinez Schramm, J., and Reimann, B., "Aerothermodynamic Investigation of the Pre-X Configuration in HEG," *New Results in Numerical and Experimental Fluid Mechanics VI*, edited by C. Tropea, S. Jakirlic, H.-J. Heinemann, Henke, R., and , H. Hönlinger, Springer, New York, 2006, pp. 229–235.

[19] Heufer, K. A., "Untersuchungen zur Filmkühlung in Supersonischen Strömungen," Ph.D. Thesis, Fakultät für Maschinenwesen der Rheinisch, Westfälischen Technischen Hochschule Aachen, Germany, 2008 (in German).

[20] Schlichting, H., and Gersten, K., "Boundary Layer Theory," 8th ed., Springer, Berlin, 2000.

[21] Florio, J., Henderson, J. B., and Test, F. L., "Experimental Determination of Volumetric Heat Transfer Coefficients in Decomposing Polymer Composites," *Porous Media, Mixtures and Multiphase Heat Transfer* (ASME Winter Annual Meeting, San Francisco, CA), HTD-Vol. 117, 1989, pp. 51–60.

[22] Innocentini, M. D. M., Rizzi, A. C., Nascimento, L. A., and Pandolfelli, V. C., "The Pressure-Decay Technique for Air Permeability Evaluation of Dense Refractory Ceramics," *Cement and Concrete Research*, Vol. 34, No. 2, 2004, pp. 293–298. doi:10.1016/j.cemconres.2003.08.006

[23] Heufer, K. A., and Olivier, H., "Experimental and Numerical Study of Cooling Gas Injection in Laminar Supersonic Flow," *AIAA Journal*, Vol. 46, No. 11, 2008, pp. 2741–2751.